

Charge-4e superconductivity from nematic superconductors in 2D and 3D

Shao-Kai Jian,¹ Yingyi Huang,² and Hong Yao^{2,3,*}

¹Condensed Matter Theory Center, Department of Physics,
University of Maryland, College Park, Maryland 20742, USA

²Institute for Advanced Study, Tsinghua University, Beijing 100084, China

³State Key Laboratory of Low Dimensional Quantum Physics, Tsinghua University, Beijing 100084, China

(Dated: June 26, 2021)

Charge-4e superconductivity as a novel phase of matter remains elusive so far. Here we show that charge-4e phase can arise as a vestigial order above the nematic superconducting transition temperature in time-reversal-invariant nematic superconductors. On the one hand, the nontrivial topological defect—nematic vortex—is energetically favored over the superconducting phase vortex when the nematic stiffness is less than the superfluid stiffness; consequently the charge-4e phase emerges by proliferation of nematic vortices upon increasing temperatures. On the other hand, the Ginzburg-Landau theory of the nematic superconductors has two distinct decoupling channels to either charge-4e orders or nematic orders; by analyzing the competition between the effective mass of the charge-4e order and the cubic potential of the nematic order, we find a sizable regime where the charge-4e order is favored. These two analysis consistently show that nematic superconductors can provide a promising route to realize charge-4e phases, which may apply to candidate nematic superconductors such as PbTaSe₂ and twisted bilayer graphene.

Introduction.—Featuring the condensation of quartets with four times the fundamental electron charges, charge-4e superconductivity [1–4] is intrinsically distinct from the conventional charge-2e superconductivity discovered more than a century ago. One hallmark of charge-4e superconductors is the magnetic flux quantization with period $hc/4e$, which is half that of the usual superconducting flux quantum. Unlike the conventional superconductivity that is well described by the seminal Bardeen–Cooper–Schrieffer (BCS) theory, many properties of charge-4e superconductivity remain less well understood. The mystery of this phase is not only because it defies any BCS-type analysis, but also due to the lack of experimental realization so far. Previous studies in Ref. [3] suggested that the charge-4e superconductivity can arise as a vestigial long-range order above the transition temperature of a pair-density-wave (PDW) superconductor [5–17], whose order parameter varies periodically in the real space. The additional breaking of translational symmetry in the PDW state is essential in realizing the charge-4e superconductivity as it provides nontrivial topological defects—dislocations. As a consequence, if the dislocation proliferates as the temperature is raised, the equilibrium state will restore the translational symmetry by doubling the original charge-2e condensate, and therefore lead to the charge-4e phase.

The crucial ingredient of the underlying condensate having more than one quantum number [18–20] provides a general guide to search for charge-4e superconductors. It was proposed that in certain two-dimensional high-temperature superconductors (e.g. La_{2–x}Ba_xCuO₄ and La_{1.6–x}Nd_{0.4}Sr_xCuO₄ [21–23]) exhibiting stripe superconducting orders [24, 25], the charge-4e superconductivity may occur above the transition temperature [3]. Nevertheless, the experimental signature of the charge-

4e superconductivity in these high-temperature superconductors has not been observed so far. Apart from PDW superconductors, the nematic superconductor that breaks both charge conservation and lattice rotational symmetry also hosts an order parameter that carries multiple quantum numbers. The additional topological defect in nematic superconductors is created by the intersection of domain walls separating different ground states. More importantly, many experimental progresses have been made in achieving the nematic superconductivity in various systems. For instance, recent experiments found that the spin susceptibility below the superconducting temperature breaks the three-fold lattice rotational symmetry in doped topological insulator Cu_xBi₂Se₃ [26–29], where the breaking of rotational symmetry suggests that the order parameter in the superconducting phase is a two-dimensional E_u representation of point group D_{3d} [30–32]. Providing the growing experimental evidence of the nematic superconductivity in various systems, including doped topological insulators Cu_xBi₂Se₃ [26–29], Sr_xBi₂Se₃ [33, 34] and Nb_xBi₂Se₃ [35, 36], superconducting topological semimetals PbTaSe₂ [37], and more recently twisted bilayer graphene [38, 39], as well as increasing interest in novel charge-4e ordering, it is thus interesting to ask whether the multiple-component superconducting order parameters in nematic superconductors is able to realize charge-4e phases above their charge-2e transition temperature.

In this paper, we answer this question in the affirmative; namely, we provide two analysis, suitable for 2D and 3D, respectively, to support the possibility of a vestigial charge-4e superconducting phase from nematic superconductors. In 2D, because a vortex is a point-like object, we analyze the fate of various topological defects to deter-

mine the phase diagram. After identifying three distinct topological defects that are responsible for three different orders out of the nematic superconducting phase, we find that the competition between the superfluid stiffness and the elastic constant leads to a rich phase diagram, as shown in Fig. 1. In particular, if the elastic constant of the material is less than one third of the superfluid stiffness, the energetically favored nematic vortices are proliferated, resulting in the novel charge-4e phase, when the temperature gets raised above the transition temperature. In 3D, we employ a Ginzburg-Landau theory near the transition point where the nematic superconducting order parameter is well described by a simple field theory up to quartic terms. We are able to show analytically that the effective mass of the charge-4e order is less than that of the nematic order by treating the three-fold anisotropy perturbatively, which indicates the charge-4e order is favored. We further confirm our results by numerically solving the saddle-point equation. Our result in 3D suggest that materials whose dispersion along the third direction is weaker than the in-plane dispersion such as in $\text{Sr}_x\text{Bi}_2\text{Se}_3$ are promising in realizing the charge-4e phase.

Charge-4e phase from proliferating topological defect.— We start by analyzing the symmetries in the nematic superconducting phase providing an appropriate language for clarifying the topological defects, and then turn to renormalization group analysis of the defect theory. As mentioned above, we consider the order parameter of the nematic superconducting phase being a two-component complex boson $\Delta = (\Delta_x, \Delta_y)^T$ carrying E_u representation in D_{3d} group, and each complex component additionally hosts the $U(1)$ quantum number corresponding to the charge conservation, i.e., it is the conventional charge-2e condensate. In the phase respecting time-reversal symmetry, the relative phase between two components Δ_x, Δ_y is pinned at 0 or π . As we focus on the time-reversal-invariant nematic superconductor, we hereafter assume the relative phase between Δ_x and Δ_y is pinned at 0 or π in the analysis of low-energy physics.

In terms of the basis $\Delta_{\pm} = \Delta_x \pm i\Delta_y$, one can bring the the four-dimensional field configuration into three phase modes and one amplitude mode. Moreover, the time reversal invariance makes one of the phase modes heavier, thus we have two phase modes and one amplitude mode in the low-energy sector,

$$\Delta_+ = |\Delta|e^{i(\theta+\phi)}, \quad \Delta_- = |\Delta|e^{i(\theta-\phi)}. \quad (1)$$

where θ and ϕ denote the two phase modes. The ϕ field describes the $U(1)$ rotation between amplitudes of two components (i.e. the spatial rotation), whereas the θ field is the $U(1)$ phase conjugated to the global charge. The two $U(1)$ phases can also be understood by secondary orders, i.e., the nematic order $Q \sim \Delta_-^\dagger \Delta_+$ and the charge-4e order $\Delta_{4e} \sim \Delta_+ \Delta_-$, that transform as

$$Q \rightarrow Qe^{2i\phi}, \quad \Delta_{4e} \rightarrow \Delta_{4e}e^{2i\theta}. \quad (2)$$

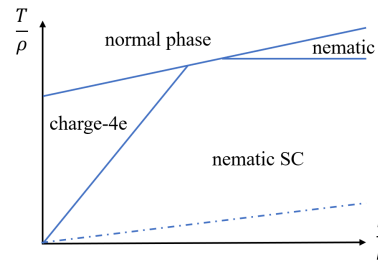


FIG. 1. Schematic phase diagram of the defect theory. κ , ρ and T denote the nematic stiffness, the superfluid stiffness and temperature, respectively. The solid lines refer to phase boundaries. Below the dashed line, the three-fold anisotropy is relevant from the lowest order calculation. Nevertheless, the true transition to the charge-4e phase belongs to the three-state Potts model universality class [40] where the three-fold anisotropy is relevant at the transition point.

The single-valueness of nematic superconducting order parameter Δ_{\pm} uniquely determines that the topological defects are given by $(\delta\theta, \delta\phi) = (2\pi, 0), (0, 2\pi), (\pi, \pi)$, where $\delta\theta, \delta\phi$ denote the winding of the phase around a defect. Physically, they correspond to the superconducting vortex, the nematic double vortex and the superconducting half-vortex binding with a single nematic vortex, respectively. In the nematic superconducting phase, the effective Hamiltonian characterizing the phase modes is

$$H = \frac{\rho}{2}(\partial\theta)^2 + \frac{\kappa}{2}(\partial\phi)^2 - g_6 \cos 6\pi\phi, \quad (3)$$

where ρ is the superfluid stiffness (superfluid density) and κ is the nematic stiffness (elastic constant). Notice that in writing this Hamiltonian, we have changed the compactification of the phase mode from 2π to 1 for convenience. Note that $\cos 6\pi\phi$ is allowed owing to the three-fold anisotropy, i.e., the action is invariant under $\phi \rightarrow \phi + 1/3$. Thermal proliferation of topological defects can be then described by the dual bosons $\tilde{\phi}$ and $\tilde{\theta}$ [3],

$$H = \frac{T}{2\rho}(\partial\tilde{\theta})^2 + \frac{T}{2\kappa}(\partial\tilde{\phi})^2 - g_6 \cos 6\pi\tilde{\phi} - g_{2,0} \cos 2\pi\tilde{\theta} - g_{0,2} \cos 2\pi\tilde{\phi} - g_{1,1} \cos \pi\tilde{\theta} \cos \pi\tilde{\phi}, \quad (4)$$

where $g_{2,0}$, $g_{0,2}$ and $g_{1,1}$ are couplings characterizing the strength of creating (annihilating) each kind of topological defects, respectively, and T is the temperature.

The standard renormalization group flow for Eq. (4) to the lowest-order reads

$$\frac{dg_{2,0}}{dl} = \left(2 - \frac{\pi\rho}{T}\right) g_{2,0}, \quad (5)$$

$$\frac{dg_{0,2}}{dl} = \left(2 - \frac{\pi\kappa}{T}\right) g_{0,2}, \quad (6)$$

$$\frac{dg_{1,1}}{dl} = \left[2 - \frac{\pi}{4T}(\rho + \kappa)\right] g_{1,1}, \quad (7)$$

$$\frac{dg_6}{dl} = \left(2 - \frac{9\pi T}{\kappa}\right) g_6. \quad (8)$$

The coefficient in front of the coupling on the right-hand side of the renormalization group equation determines whether the corresponding process is relevant or not. For instance, if $\frac{T}{\rho} > \frac{\pi}{2}$, the creation and annihilation process of the superconducting vortex is relevant, leading to the proliferation of superconducting phase defects and, consequently, destroying the superconducting phase coherence driving the system out of superconducting orders. In this way, the phase diagram as shown in Fig. 1 is mapped out by the renormalization group equations. Clearly, when the nematic stiffness is less than the superfluid stiffness, more specifically $\kappa < \frac{\rho}{3}$, it is easier to create nematic vortices than superconducting vortices such that raising temperature can more efficiently proliferate the nematic vortices, restoring the lattice rotational symmetry but not the $U(1)$ charge symmetry. As a result, the charge-4e order emerges since any charge-2e condensate from the nematic superconductivity breaks lattice rotational symmetry whereas the charge-4e order is blind to the nematic vortex as shown by the symmetry transformation law in Eq. (2).

Besides the interesting charge-4e phase, the competition between the nematic stiffness and the superfluid stiffness results in a rich phase diagram in Fig. 1. Namely, when $\frac{1}{3} < \frac{\kappa}{\rho} < 3$, raising the temperature causes a direct transition from the nematic superconductivity to the normal phase since proliferating a superconducting half-vortex bounded with a nematic vortex is favored, whereas, when $\frac{\kappa}{\rho} > 3$, a vestigial of nematic phase emerges since proliferating the normal superconducting phase vortex is favored [41].

Charge-4e phase from superconducting fluctuations.— In 3D, the Ginzburg-Landau theory works better since the quantum fluctuation is generally suppressed as dimension increases, so we expect a mean-field analysis to 3D nematic superconductivity near the phase boundary can describe the essential physics. Such a theory was also used in Ref. [32] to investigate the vestigial nematic order, but the authors did not analyze the possibility of charge-4e orders. The Ginzburg-Landau theory of the nematic superconducting order parameter $\Delta = (\Delta_x, \Delta_y)^T$ near the phase boundary reads [32]

$$S = \int_p \Delta^\dagger G_p^{-1} \Delta + \int_x (u(\Delta^\dagger \Delta)^2 + v(\Delta^\dagger \tau^y \Delta)^2), \quad (9)$$

where $\int_p = \int \frac{d^3p}{(2\pi)^3}$, $\int_x = \int d^3x$, and

$$G_p^{-1} = m_0(\mathbf{p})\tau^0 + m_1(\mathbf{p})\tau^z + m_2(\mathbf{p})\tau^x, \quad (10)$$

is the inverse propagator of the nematic superconducting order parameter with $m_0(\mathbf{p}) = d_{\parallel}(p_x^2 + p_y^2) + d_z p_z^2 + r_0$, $m_1(\mathbf{p}) = d'(p_x^2 - p_y^2) + \bar{d}p_y p_z$, and $m_2(\mathbf{p}) = d'2p_x p_y + \bar{d}p_x p_z$. Notice that while $m_0(\mathbf{p})$ enjoys a continuous rotational symmetry, $m_1(\mathbf{p})$ and $m_2(\mathbf{p})$ lower it down to three-fold rotation. r_0, u, v are real parameters allowed by the symmetry and $d_{\parallel}, d_z, d', \bar{d}$ characterize the kinetic

energy. In the following, we consider $v > 0, u > 0$, as the case for $v < 0$ favors the chiral superconductivity that breaks time reversal symmetry. It is crucial to realize that there are two ways given by the following two different Fierz identities to decouple the last quartic term in Eq. (9)

$$\tau_{\alpha\beta}^y \tau_{\gamma\delta}^y = 2\delta_{\alpha\delta} \delta_{\beta\gamma} - \delta_{\alpha\beta} \delta_{\gamma\delta} - \tau_{\alpha\beta}^x \tau_{\gamma\delta}^x - \tau_{\alpha\beta}^z \tau_{\gamma\delta}^z, \quad (11)$$

$$\tau_{\alpha\beta}^y \tau_{\gamma\delta}^y = \delta_{\alpha\beta} \delta_{\gamma\delta} - \delta_{\alpha\gamma} \delta_{\beta\delta}. \quad (12)$$

This leads to either nematic channel for the first one Eq. (11) or charge-4e channel for the second one Eq. (12). After the decoupling, one is able to integrate out the quadratic nematic superconducting order parameter. We leave the details to the Supplemental Materials [42], and present the main results here. The Ginzburg-Landau theory for the nematic order and the charge-4e order (assuming to be homogeneous in real space) are given by

$$S_{nem} = \text{Tr} \log \chi_p^{-1} + \int_x \left(\frac{1}{4v}(Q_x^2 + Q_y^2) - \frac{1}{4u'}R^2 \right), \quad (13)$$

$$S_{4e} = \frac{1}{2} \text{Tr} \log D_p^{-1} + \int_x \left(\frac{1}{4v}|\Delta_{4e}|^2 - \frac{1}{4u'}R^2 \right), \quad (14)$$

where $u' = u + v$, Q_x, Q_y are the nematic orders, Δ_{4e} is the charge-4e order, and $R \sim \Delta^\dagger \Delta$ is a scalar that decouples the first quartic interaction in Eq. (9). The $\text{Tr} \log$ term comes from integrating out the nematic superconducting order parameter, and $\chi_p^{-1} = G_p^{-1} + R + Q_x \tau^z + Q_y \tau^x$, and $D_p^{-1} = G_p^{-1} + R + \Delta_{4e} \rho^+ + \Delta_{4e}^* \rho^-$ are the modified inverse propagators in the presence of the nematic order and the charge-4e order, respectively. $\rho^\pm = \frac{1}{2}(\rho^x \pm i\rho^y)$ where ρ^x and ρ^y are Pauli matrices acting on the ‘‘Nambu’’ space, i.e., Δ_{4e} and Δ_{4e}^* , and the extra factor $\frac{1}{2}$ in front of the $\text{Tr} \log$ term in Eq. (14) is due to the redundancy of the enlarged Nambu space.

The Fierz identity and the bosonic nature of the nematic superconducting order parameter Δ cause the similar Ginzburg-Landau theory for the nematic order Eq. (13) and the charge-4e orders Eq. (14). The only difference comes from the $\text{Tr} \log$ term as the nematic order carries a real space (nematic) quantum number while the charge-4e order carries a Nambu space quantum number. Unlike the fermionic field, the bosonic nematic superconducting field is blind to the Nambu space as one can easily observe that the inverse propagator G_p^{-1} (10) is an identity in the Nambu space. Thus if one artificially turns off m_1 and m_2 such that the nematic superconducting field has an accidental continuous real space rotational symmetry at the leading order, the nematic order and the charge-4e order will be degenerate since now the nematic superconducting field is blind to both nematic space and Nambu space (the factor of $\frac{1}{2}$ in Eq. (14) is perfectly compensated by the enlarged Nambu space). So even without any calculation, one can identify a specific albeit artificial point where the charge-4e order is degenerate with

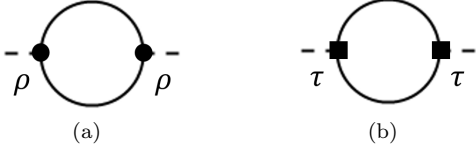


FIG. 2. The Feynman diagrams that contribute to the effective mass of the charge-4e order and the nematic order, respectively. The difference of (a) and (b) arises from the different vertices denoted by ρ and τ .

the nematic order. Now the question is how the non-vanishing m_1 and m_2 , equivalently d' and \bar{d} , affect the two instabilities. In the following, we provide an analytical result showing the charge-4e order is favored over the nematic order when $d' \gg \bar{d}$, which makes quasi-2D materials whose out-of-plane dispersion is much weaker than the in-plane dispersion promising candidates for realizing charge-4e phases. In addition, we also numerically solve the saddle-point equation for both nematic orders and charge-4e orders, which confirms the analytical result.

Near the transition point, the effective Ginzburg-Landau theory can be obtained by assuming order parameters small and expanding the action order by order. The effective mass that is crucial in determining the phase boundary is given by evaluating the Feynman diagram in Fig. 2, and as we discussed above the difference lies in the vertices of the two orders as shown in Fig. 2(a) and Fig. 2(b). Since nonvanishing m_1 and m_2 are diagonal in the Nambu space the contributions from the τ^z and τ^x kinetic energy are additive to the charge-4e order's mass; however, since they are not diagonal in the nematic space the contributions tend to cancel each other. We calculate the effective mass perturbatively in \bar{d} , and the lowest-order result is

$$m_{4e} = m_{nem} - \delta m_2, \quad (15)$$

$$\delta m_2 = \frac{1}{d_{\parallel} \sqrt{d_z(R+r_0)}} \frac{2\gamma - (1-\gamma^2) \log\left(\frac{1+\gamma}{1-\gamma}\right)}{32\pi\gamma(1-\gamma^2)}, \quad (16)$$

where $\gamma = \frac{d'}{d_{\parallel}}$. It is not hard to see that δm_2 is positive and monotonic in $0 < \gamma < 1$, indicating the anisotropy induced by nonvanishing d' favors the charge-4e order.

However, this enhancement of the charge-4e instability needs to compete with the cubic potential of nematic orders arising from the three-fold anisotropy. The cubic term appears at least at the quadratic order in \bar{d} and the linear order in d' (actually, the dependence of d' at quadratic order of \bar{d} can be obtained explicitly), and through explicit calculation, the cubic term is

$$S_{nem} \ni w \int (Q_x^3 - 3Q_x Q_y^2), \quad (17)$$

$$w \approx \frac{1}{960\pi} \frac{1}{[d_z(R+r_0)]^{3/2}} \frac{\bar{d}^2 d'}{d_{\parallel}^3}. \quad (18)$$

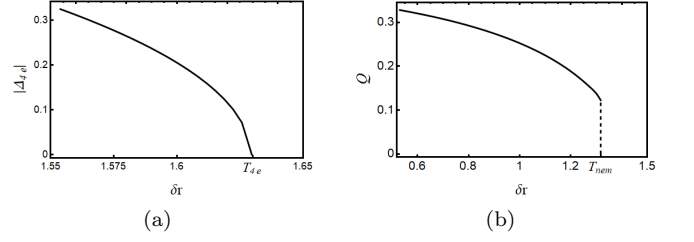


FIG. 3. The mean field phase diagram of the charge-4e order (a) and the nematic order (b). $|\Delta_{4e}|$, and $Q = \sqrt{Q_x^2 + Q_y^2}$ are the amplitude of the charge-4e and the nematic order respectively. $\delta r = r_0 - r_0^* \propto T - T^*$, where r^* (T^*) denotes the transition point (transition temperature) without vestigial orders. The parameters are $d_{\parallel} = 1$, $d' = 0.5$, $d_z = 0.1$, $\bar{d} = 0.1$, $v = 1$, $u = 4$.

It is a simple matter of fact that the cubic term enhances the instability at least in the quadratic orders, i.e., $\delta m_3 \propto w^2 \propto \bar{d}^4$, so the lowest order is the quartic order in \bar{d} . On the other hand, the enhancement of the charge-4e superconductivity δm_2 appears already in the zeroth order of \bar{d} . For the systems described by Eq. (9), there exists a parameter regime, where $\bar{d} \ll d'$, such that the charge-4e order is favored over the nematic order. Notice that we have neglected the sixth order terms like $(\Delta^\dagger(\tau^z + i\tau^x)\Delta)^3 + h.c.$ in Eq. (9) that are allowed by the three-fold anisotropy, and these terms can also render cubic contributions to the nematic order effective action Eq. (17). These higher order terms are in general irrelevant for the long wavelength physics near and slightly above the nematic superconducting transition temperature at which the Ginzburg-Landau theory Eq. (9) can apply. (Whereas if the temperature is lower than the transition temperature, this becomes dangerously irrelevant [15] and selects one of the degenerate ground states). Unlike the universal physics that can be obtained with the help of the Ginzburg-Landau action in Eq. (9), it is not clear away from the applicability of such an action what the fate of the competition between the charge-4e order and the nematic order is. Nevertheless, the 2D calculation shown in Fig. 1 provides a complementary qualitative understanding: the large anisotropy from higher-order potentials can increase the nematic stiffness and prohibit the charge-4e phase [41].

To further support our result, we carry out a numerical calculation of the saddle-point equations in both the charge-4e channel and the nematic channel. We leave the saddle-point equation in the Supplemental Materials [42]. The phase diagram is shown in Fig. 3, where $|\Delta_{4e}|$, and $Q = \sqrt{Q_x^2 + Q_y^2}$ are the amplitude of the charge-4e and the nematic order respectively. $\delta r = r_0 - r_0^* \propto T - T^*$, where r^* (T^*) denotes the transition point (transition temperature) without vestigial orders. That the system is in favor of the charge-4e phases when $\bar{d} \ll d'$ is demon-

strated explicitly by $T_{nem} < T_{4e}$ in Fig. 3. One should also notice the first-order jump of the nematic transition due to the cubic anisotropy, on the contrary, the phase transition to the nematic phase at two dimensions is continuous due to the strong quantum fluctuations [40].

Conclusions.—We have revealed the promising possibility of realizing a novel charge-4e superconducting phase above the transition temperature of time-reversal-invariant nematic superconductors in 2D and quasi-2D. Since experimental evidences of rotational symmetry breaking superconducting phases in various systems, including doped topological insulators $\text{Cu}_x\text{Bi}_2\text{Se}_3$ [26–29], $\text{Sr}_x\text{Bi}_2\text{Se}_3$ [33, 34], and $\text{Nb}_x\text{Bi}_2\text{Se}_3$ [35, 36], superconducting topological semimetal PbTaSe_2 [37], and more recently twisted bilayer graphene [38, 39], have accumulated, we believe that our results pave an important step toward experimentally realizing charge-4e phases in quantum materials.

Acknowledgement.— We thank Wen Huang for helpful discussions. This work is supported in part by the NSFC under Grant No. 11825404 (HY), the MOSTC under Grant Nos. 2016YFA0301001 and 2018YFA0305604 (HY), and the Strategic Priority Research Program of Chinese Academy of Sciences under Grant No. XDB28000000 (HY). SKJ is supported by the Simons Foundation via the It From Qubit Collaboration.

Note added: While the present paper was close to be completed, we notice an interesting work on a similar topic in Ref. [43]. Our results of Ginzburg-Landau theory analysis in three dimensions are qualitatively consistent with ones in Ref. [43]. We additionally analyzed the topological defect theory in two dimensions which supports the possibility of realizing charge-4e phase.

* yaohong@tsinghua.edu.cn

- [1] S. Kivelson, V. Emery, and H. Lin, Phys. Rev. B **42**, 6523 (1990).
- [2] C. Wu, Phys. Rev. Lett. **95**, 266404 (2005).
- [3] E. Berg, E. Fradkin, and S. A. Kivelson, Nature Physics **5**, 830 (2009).
- [4] Y.-F. Jiang, Z.-X. Li, S. A. Kivelson, and H. Yao, Phys. Rev. B **95**, 241103 (2017).
- [5] P. Fulde and R. A. Ferrell, Phys. Rev. **135**, A550 (1964).
- [6] A. Larkin and Y. N. Ovchinnikov, JETP **20**, 762 (1965).
- [7] L. Radzihovsky and A. Vishwanath, Phys. Rev. Lett. **103**, 010404 (2009).
- [8] D. Agterberg and H. Tsunetsugu, Nature Physics **4**, 639 (2008).
- [9] C. Wang, C. Gao, C.-M. Jian, and H. Zhai, Phys. Rev. Lett. **105**, 160403 (2010).
- [10] G. Y. Cho, J. H. Bardarson, Y.-M. Lu, and J. E. Moore, Phys. Rev. B **86**, 214514 (2012).
- [11] P. A. Lee, Phys. Rev. X **4**, 031017 (2014).
- [12] J. Maciejko and R. Nandkishore, Phys. Rev. B **90**, 035126 (2014).
- [13] S.-K. Jian, Y.-F. Jiang, and H. Yao, Phys. Rev. Lett. **114**, 237001 (2015).
- [14] S.-K. Jian, C.-H. Lin, J. Maciejko, and H. Yao, Phys. Rev. Lett. **118**, 166802 (2017).
- [15] S.-K. Jian, M. M. Scherer, and H. Yao, Phys. Rev. Research **2**, 013034 (2020).
- [16] Z. Han, S. A. Kivelson, and H. Yao, Phys. Rev. Lett. **125**, 167001 (2020).
- [17] D. F. Agterberg, J. S. Davis, S. D. Edkins, E. Fradkin, D. J. Van Harlingen, S. A. Kivelson, P. A. Lee, L. Radzihovsky, J. M. Tranquada, and Y. Wang, Annual Review of Condensed Matter Physics **11**, 231 (2020).
- [18] S. B. Chung, S. Raghu, A. Kapitulnik, and S. A. Kivelson, Physical Review B **86**, 064525 (2012).
- [19] E.-G. Moon, Phys. Rev. B **85**, 245123 (2012).
- [20] C. Xu and L. Balents, Physical review letters **121**, 087001 (2018).
- [21] M. Fujita, H. Goka, K. Yamada, J. Tranquada, and L. Regnault, Phys. Rev. B **70**, 104517 (2004).
- [22] J. M. Tranquada, G. D. Gu, M. Hücker, Q. Jie, H.-J. Kang, R. Klingeler, Q. Li, N. Tristan, J. S. Wen, G. Y. Xu, Z. J. Xu, J. Zhou, and M. v. Zimmermann, Phys. Rev. B **78**, 174529 (2008).
- [23] M. Hücker, M. v. Zimmermann, G. Gu, Z. Xu, J. Wen, G. Xu, H. Kang, A. Zheludev, and J. M. Tranquada, Phys. Rev. B **83**, 104506 (2011).
- [24] E. Berg, E. Fradkin, E.-A. Kim, S. A. Kivelson, V. Oganesyan, J. M. Tranquada, and S.-C. Zhang, Phys. Rev. Lett. **99**, 127003 (2007).
- [25] E. Berg, E. Fradkin, and S. A. Kivelson, Phys. Rev. B **79**, 064515 (2009).
- [26] K. Matano, M. Kriener, K. Segawa, Y. Ando, and G.-q. Zheng, Nature Physics **12**, 852 (2016).
- [27] S. Yonezawa, K. Tajiri, S. Nakata, Y. Nagai, Z. Wang, K. Segawa, Y. Ando, and Y. Maeno, Nature Physics **13**, 123 (2017).
- [28] R. Tao, Y.-J. Yan, X. Liu, Z.-W. Wang, Y. Ando, Q.-H. Wang, T. Zhang, and D.-L. Feng, Phys. Rev. X **8**, 041024 (2018).
- [29] S. Yonezawa, Condensed Matter **4**, 2 (2019).
- [30] L. Fu, Phys. Rev. B **90**, 100509 (2014).
- [31] J. W. Venderbos, V. Kozii, and L. Fu, Phys. Rev. B **94**, 180504 (2016).
- [32] M. Hecker and J. Schmalian, npj Quantum Materials **3**, 1 (2018).
- [33] J. Wang, K. Ran, S. Li, Z. Ma, S. Bao, Z. Cai, Y. Zhang, K. Nakajima, S. Ohira-Kawamura, P. Čermák, A. Schneidewind, S. Y. Savrasov, X. Wan, and J. Wen, Nature communications **10**, 2802 (2019).
- [34] I. Kostylev, S. Yonezawa, Z. Wang, Y. Ando, and Y. Maeno, Nature communications **11**, 1 (2020).
- [35] J. Shen, W.-Y. He, N. F. Q. Yuan, Z. Huang, C.-w. Cho, S. H. Lee, Y. San Hor, K. T. Law, and R. Lortz, npj Quantum Materials **2**, 1 (2017).
- [36] T. Asaba, B. Lawson, C. Tinsman, L. Chen, P. Corbae, G. Li, Y. Qiu, Y. S. Hor, L. Fu, and L. Li, Physical Review X **7**, 011009 (2017).
- [37] T. Le, Y. Sun, H.-K. Jin, L. Che, L. Yin, J. Li, G. Pang, C. Xu, L. Zhao, S. Kittaka, T. Sakakibara, K. Machida, R. Sankar, H. Yuan, G. Chen, X. Xu, S. Li, Y. Zhou, and X. Lu, Science Bulletin **65**, 1349 (2020).
- [38] A. Kerelsky, L. J. McGilly, D. M. Kennes, L. Xian, M. Yankowitz, S. Chen, K. Watanabe, T. Taniguchi, J. Hone, C. Dean, A. Rubio, and A. N. Pasupathy, Nature **572**, 95 (2019).

- [39] Y. Cao, D. Rodan-Legrain, J. M. Park, F. N. Yuan, K. Watanabe, T. Taniguchi, R. M. Fernandes, L. Fu, and P. Jarillo-Herrero, arXiv:2004.04148 (2020).
 [40] F.-Y. Wu, Rev. Mod. Phys. **54**, 235 (1982).
 [41] C.-w. Cho, J. Shen, J. Lyu, O. Atanov, Q. Chen, S. H. Lee, Y. San Hor, D. J. Gawryluk, E. Pomjakushina,

M. Bartkowiak, *et al.*, Nature communications **11**, 1 (2020).

- [42] See Supplemental Materials for the technical details of derivation the saddle-point equation.
 [43] R. M. Fernandes and L. Fu, arXiv:2101.07943 (2021).

Supplemental Materials

There are two ways to decouple the quartic term in Eq. (9), given by the following two different Fierz identities

$$\tau_{\alpha\beta}^y \tau_{\gamma\delta}^y = 2\delta_{\alpha\delta} \delta_{\beta\gamma} - \delta_{\alpha\beta} \delta_{\gamma\delta} - \tau_{\alpha\beta}^x \tau_{\gamma\delta}^x - \tau_{\alpha\beta}^z \tau_{\gamma\delta}^z, \quad (\text{S1})$$

$$\tau_{\alpha\beta}^y \tau_{\gamma\delta}^y = \delta_{\alpha\beta} \delta_{\gamma\delta} - \delta_{\alpha\gamma} \delta_{\beta\delta}, \quad (\text{S2})$$

which lead to two exact rewritings of Eq. (9)

$$S = \int_p \Delta^\dagger G_p^{-1} \Delta + \int_x (u' (\Delta^\dagger \Delta)^2 - v [(\Delta^\dagger \tau^x \Delta)^2 + (\Delta^\dagger \tau^z \Delta)^2]), \quad (\text{S3})$$

$$S = \int_p \Delta^\dagger G_p^{-1} \Delta + \int_x (u' (\Delta^\dagger \Delta)^2 - v |\Delta^T \Delta|^2), \quad (\text{S4})$$

where $u' = u + v$.

The first equation (S3) is readily decoupled by nematic orders, (Q_x, Q_y) ,

$$S = \int_x \left(\Delta^\dagger (G^{-1} + R + Q_x \tau^z + Q_y \tau^x) \Delta + \frac{1}{4v} (Q_x^2 + Q_y^2) - \frac{1}{4u'} R^2 \right), \quad (\text{S5})$$

where R is another boson field that decouple u' term, and it does not break any symmetry. On the other hand, the second equation (S4) is readily decoupled by charge-4e SC orders, $(\Delta_{4e}, \Delta_{4e}^*)$,

$$S = \int_x \left(\frac{1}{2} \hat{\Delta}^\dagger \begin{pmatrix} G^{-1} + R & \Delta_{4e} \\ \Delta_{4e}^* & G^{-1} + R \end{pmatrix} \hat{\Delta} + \frac{1}{4v} |\Delta_{4e}|^2 - \frac{1}{4u'} R^2 \right) \quad (\text{S6})$$

where $\hat{\Delta} = (\Delta^\dagger, \Delta^T)$.

Since now the nematic SC order is quadratic in the action, it is straightforward to integrate it over.

$$S = \text{Tr} \log(G^{-1} + R + Q_x \tau^z + Q_y \tau^x) + \int_x \left(\frac{1}{4v} (Q_x^2 + Q_y^2) - \frac{1}{4u'} R^2 \right), \quad (\text{S7})$$

$$S = \frac{1}{2} \text{Tr} \log \begin{pmatrix} G^{-1} + R & \Delta_{4e} \\ \Delta_{4e}^* & G^{-1} + R \end{pmatrix} + \int_x \left(\frac{1}{4v} |\Delta_{4e}|^2 - \frac{1}{4u'} R^2 \right). \quad (\text{S8})$$

From the effective action (13), the saddle-point equation for homogeneous nematic orders, $Q_i(\mathbf{x}) = Q_i$, $i = x, y$ reads

$$R = 2u' \Delta_0^\dagger \Delta_0 + 2u' \int_p \text{Tr}(G_p^{-1} + R + Q_x \tau^z + Q_y \tau^x)^{-1}, \quad (\text{S9})$$

$$Q_x = -2v \Delta_0^\dagger \tau^z \Delta_0 - 2v \int_p \text{Tr}(G_p^{-1} + R + Q_x \tau^z + Q_y \tau^x)^{-1} \tau^z, \quad (\text{S10})$$

$$Q_y = -2v \Delta_0^\dagger \tau^x \Delta_0 - 2v \int_p \text{Tr}(G_p^{-1} + R + Q_x \tau^z + Q_y \tau^x)^{-1} \tau^x, \quad (\text{S11})$$

$$0 = \chi_0^{-1} \Delta_0. \quad (\text{S12})$$

On the other hand, the saddle-point equation for homogeneous charge-4e SC orders $\Delta_{4e}(\mathbf{x}) = \Delta'_{4e} + i\Delta''_{4e}$ where

$\Delta'_{4e}, \Delta''_{4e} \in \mathbb{R}$ from Eq. (14) reads

$$R = 2u' \Delta_0^\dagger \Delta_0 + u' \int_p \text{Tr} \left(\begin{array}{cc} G_p^{-1} + R & \Delta'_{4e} + i\Delta''_{4e} \\ \Delta'_{4e} - i\Delta''_{4e} & G_p^{-1} + R \end{array} \right)^{-1} \quad (\text{S13})$$

$$\Delta'_{4e} = -2v \text{Re}[\Delta_0^T \Delta_0] - v \int_p \text{Tr} \left(\begin{array}{cc} G_p^{-1} + R & \Delta'_{4e} + i\Delta''_{4e} \\ \Delta'_{4e} - i\Delta''_{4e} & G_p^{-1} + R \end{array} \right)^{-1} \rho^x, \quad (\text{S14})$$

$$\Delta''_{4e} = -2v \text{Im}[\Delta_0^T \Delta_0] - v \int_p \text{Tr} \left(\begin{array}{cc} G_p^{-1} + R & \Delta'_{4e} + i\Delta''_{4e} \\ \Delta'_{4e} - i\Delta''_{4e} & G_p^{-1} + R \end{array} \right)^{-1} (-\rho^y), \quad (\text{S15})$$

$$0 = \chi_0^{-1} \Delta_0. \quad (\text{S16})$$

In the saddle-point equations, we also assume $R(\mathbf{x}) = R$ is homogeneous. The saddle-point equations are solved numerically, and the results are shown in Fig. 3.